

Generation of a Smooth Ostium Surface for Aneurysm Surface Models

Mathias Neugebauer¹, Bernhard Preim¹

¹Department of Simulation and Graphics, Otto-von-Guericke Universität Magdeburg
`mathias.neugebauer@ovgu.de`

Abstract. The exploration of the complex flow patterns within cerebral aneurysms is crucial for risk assessment, therapy planning and medical research. In order to support visual exploration, geometric descriptors are necessary to decompose the complex flow data. An important descriptor is the ostium, the area of inflow into the aneurysm, since other descriptors can be derived from it. We describe an interpolation-based approach to generate a smooth ostium surface that was successfully applied to seven different aneurysm surface models.

1 Introduction

A cerebral aneurysm is a pathological artery dilatation and forms an area with a high risk of rupture. Insight into intravascular flow characteristics is important for risk assessment, therapy planning and comparison of treatment options (e.g. different stents and their placement) as well as the development of new, minimal invasive treatment techniques. A way to retrieve this kind of data is a CFD simulation, based on 3D reconstructions of the affected vessel. The resulting flow data is complex and a subdivision into functional unities supports the visual exploration. Since blood flow is mainly influenced by the surrounding vascular geometry [1], this subdivision should be derived from geometric landmarks. An important landmark is the ostium, the area of inflow into the aneurysm. Based on this landmark, the aneurysm can be separated from the unaffected parts of the parent vessel. Additional geometric descriptors (dome, central axis, axes of minimal and maximum extent, etc.) can be calculated if the ostium is known. They are important for quantification and characterization of the corresponding parts of the flow field and for a general support of the visual exploration (adapted visualization, viewpoint selection, meaningfully restricted degrees of freedom during navigation, etc.).

In [2] the angle between the parent vessel bifurcation and the aneurysm neck plane was quantified. However, they did not explicitly reconstruct the ostium. Karmonik et al. [3] applied an image-based approach by fitting circles to the cross section of the parent vessel. This approach is error-prone, if the vessel strongly deviates from a tubular shape, which is often the case close to the aneurysm. To avoid this problem, our approach to generate a surface representation of the ostium is based on landmarks that were derived from the aneurysm surface, rather than from within the parent vessel.

2 Methods

The generation of the ostium surface is a two step approach: Shape features are generated which subsequently form the input for a smooth sampling of the ostium surface by means of interpolation. Some of the shape features are created during the pre-processing whereas others are explicitly computed to meet the requirements of the final ostium surface shape.

2.1 Input Data

Anatomically the ostium describes the area of inflow into the aneurysm. In most of the cases, flow data is calculated on a CFD-compliant volume-mesh. We derive the ostium surface from this mesh as well. A detailed description of the segmentation process, that is necessary to derive a volume mesh from the image data, is beyond the scope of this work. We refer to [4] who segment cerebral aneurysms from PCMRA¹ data utilizing multi range filters and local variances and to [5] who apply geometric deformable models to CTA² and 3DRA³ data.

Besides the surface of the volume mesh we need two more inputs: the parent vessel centerline and a contour that describes the location of the ostium with respect to the surface (see Fig. 2(a)). The parent vessel centerline is also derived from the surface of the volume mesh, utilizing its Voronoi diagram. A robust implementation is given as part of the Vascular Modeling Toolkit (VMTK) [2]. The ostium contour (C_O) is constructed geometrically as a result of an iterative process that utilizes the parent vessel centerline and the surface as input. Starting from an estimated dome point of the aneurysm four control points are shifted towards the parent vessel. Model assumptions (the ostium is bent around the parent vessel, it is always oriented towards the aneurysm [6]) need to be satisfied during this process. Finally, two of the control points (P_1, P_2) are placed on the parent vessel, at the transition zone between parent vessel and aneurysm. The remaining control points (P_3, P_4) lie in between them and describe the bending. The smooth ostium contour is formed by a closed spline going through all control points ($P_1 - P_4$). In [6] this process is described in detail.

2.2 Shape Features for the Ostium Surface

The ostium contour C_O and a part of the parent vessel centerline that is projected into the ostium area are the shape features of the ostium surface. These features enable us to generate a closed surface in between. The outer border of the surface is already given by the ostium contour C_O through $P_1 - P_4$ (see Fig. 2(a)). The projection of the centerline, going through P_1 and P_2 , ensures that the ostium surface adjusts to the location and the bending of the underlying parent-vessel (see Fig. 1(a)).

¹ Phase Contrast Magnetic Resonance Angiography

² Computed Tomography Angiography

³ 3D Rotational Angiography

Centerline Correction: Beneath the ostium the centerline tends to bulge into the aneurysm (see Fig. 1(a)), since the surface in this area deviates from the tubular shape given in the parent vessel. This part of the parent vessel centerline needs to be corrected. First we identify the last reliable parts of the centerline within the parent vessel, before and after the aneurysm. Each of these parts is defined by two points (a_1, a_2) on the centerline that have minimal distances to P_1 and P_2 (b_1, b_2) respectively. These four points are used as control points for a cubic Lagrange polynomial that will replace the unreliable part of the centerline. The parameterization t for each point is $t(a_1) = 0.0$, $t(a_2) = \omega$, $t(a_3) = 1.0 - \omega$, $t(a_4) = 1.0$ where ω is defined by:

$$\omega = \left(\|\overrightarrow{a_1 a_2}\| + \|\overrightarrow{b_1 b_2}\| \right) / \left(2 \cdot \|\overrightarrow{a_1 b_2}\| \right)$$

The Lagrange approximation algorithm is used to sample the polynomial and the original centerline points are replaced with the samples.

Centerline Projection: The corrected centerline is projected into to ostium area by interpolating between the vectors $\overrightarrow{v_1} = \overrightarrow{P_1 a_2}$ and $\overrightarrow{v_2} = \overrightarrow{P_2 b_1}$ (see Fig. 1(a)). For each point p_i of the n centerline points between a_2 and b_1 the projected point p'_i is defined by:

$$p'_i = p_i + \left(1 - \frac{i}{n} \right) \overrightarrow{v_1} + \left(\frac{i}{n} \right) \overrightarrow{v_2}$$

The projected centerline (C_P) starts from P_1 , resembles the shape of the underlying parent-vessel centerline and ends at P_2 .

2.3 Surface Generation

The projected centerline C_P divides the ostium surface, we want to generate, into two parts. Without loss of generality we describe the surface generation process for only one of these parts, since it is a local approach that can be applied to both parts separately.

We subdivide the segment of ostium contour C_O that is contained in the chosen part into two segments C_a and C_b of equal geodesic length. The two segments share the division point p_d and are uniformly sampled with the same number of samples k . The surface is generated by linear interpolation from C_a to C_b . For this, we need a suitable interpolation path. This path is given by linear segments $L_1 - L_j$ that are defined between the j points of the projected centerline C_P and p_d . Each segment L_i is sampled uniformly and has the same number of samples k as the contour segments. For the first linear segment L_1 , a set of vectors V_a is defined by $\overrightarrow{V_{ai}} = \overrightarrow{L_{1i} C_{ai}}$, where L_{1i} is the sample on L_1 and C_{ai} is the corresponding sample on C_a . The same is done for the last linear segment L_j and C_b with the vector set V_b as result (see Fig. 1(b)).

We now have a set of vectors V_a that is related to C_a and a set V_b that is related to C_b respectively. The j linear segments with k samples each define

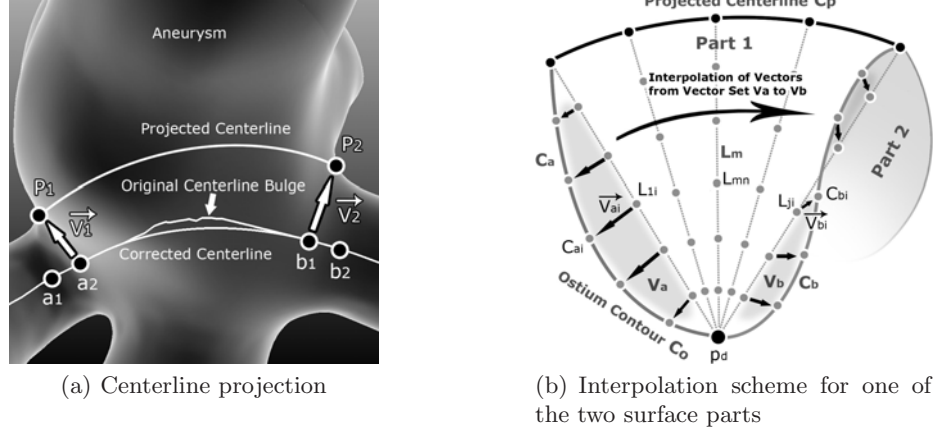


Fig. 1. The projection of the corrected centerline is one input for the surface generation.

the sampling of our surface. For each sample point $L_m n$, with $0 \leq m < j$ and $0 \leq n < k$, we define a displacement that includes the linear interpolation from V_a to V_b :

$$L'_{mn} = L_{mn} + \left(1 - \frac{m}{j}\right) \vec{V}_{an} + \left(\frac{m}{j}\right) \vec{V}_{bn}$$

The regular $j \times k$ structure of the sample point allows us to use simple, vertex Id-based construction rules to define the topology based on the displaced sampling points. The result is a mesh that smoothly interpolates the geometric constraints given by C_O (represented by C_a, C_b) and C_P (represented by $L_1 - L_j$) (see Fig. 2(b)).

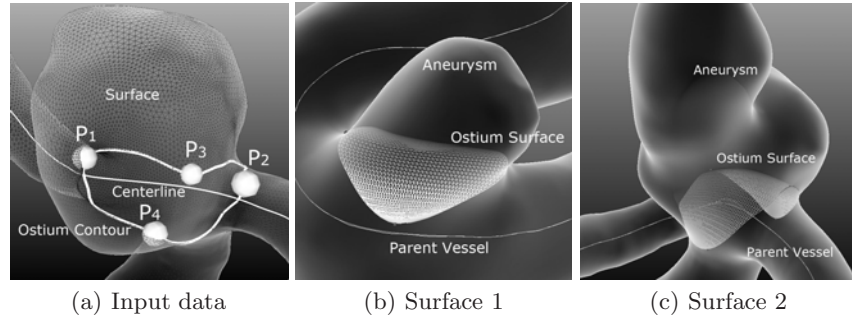


Fig. 2. The input data and two examples of generated ostium surfaces (images from three different datasets).

3 Results and Discussion

We used MEVISLAB 2.1 as prototyping environment, since it wraps the Visualization Toolkit (VTK) whose mesh processing and visualization capabilities form the basis of our implementation. As input data seven different polygonal models were derived from different imaging devices (CTA/MRA) during clinical standard procedures. The centerlines of the parent vessels were calculated using VMTK and used as input for the generation of the ostium contours [6]. The ostium surface could be generated successfully for all ostium contours. On a mid-class laptop the computation time for a high-resolution ostium surface (4096 sample points) on different datasets was in between 0.8 and 1.1 *sec* with a non-optimized, straightforward implementation. Besides a small overhead for preprocessing (projection of the centerline, subdividing the contour into C_a , C_b) the computation time depends linearly on the surface resolution.

The resulting ostium surfaces are smooth and bend natural according to the underlying parent vessel and the aneurysm-vessel transition area (see Fig. 2(b),2(c)). Medical experts found them to be plausible and correctly related to the particular morphologic situation. Using this ostium surface, the next step is to generate an aneurysm-specific coordinate system that includes the semantic decomposition of the aneurysm (ostium, neck, dome) and special geometric landmarks and axes. This coordinate system will form the basis for adaptable visualizations and support the visual exploration process.

Acknowledgment: This work has been funded by the federal state of Saxony-Anhalt in the scope of the MOBESTAN project (5161AD/0308M).

References

1. Tateshima S, Chien A, Sayre J, Cebal J, Vinuela F. The effect of aneurysm geometry on the intra-aneurysmal flow condition. *Neuroradiology*. 2010;ePub. Available from: <http://www.biomedsearch.com/nih/effect-aneurysm-geometry-intra-aneurysmal/20373097.html>.
2. Piccinelli M, Veneziani A, Steinman DA, Remuzzi A, Antiga L. A framework for geometric analysis of vascular structures: Application to cerebral aneurysms. *Medical Imaging, IEEE Transactions on*. 2009;28(8):1141–1155.
3. Karmonik C, Arat A, Benndorf G, Akpek S, Klucznik R, Mawad ME, et al. A technique for improved quantitative characterization of intracranial aneurysms. *American Journal of Neuroradiology*. 2004;25(7):1158–1161.
4. Law M, Chung A. Vessel and Intracranial Aneurysm Segmentation Using Multi-range Filters and Local Variances. *Medical Image Computing and Computer-Assisted Intervention–MICCAI 2007*. 2007; p. 866–874.
5. Hernandez M, Frangi AF. Non-parametric geodesic active regions: Method and evaluation for cerebral aneurysms segmentation in 3DRA and CTA. *Medical Image Analysis*. 2007;11(3):224–241.
6. Neugebauer M, Diehl V, Skalej M, Preim B. Geometric Reconstruction of the Ostium of Cerebral Aneurysms. In: Koch R, Kolb A, Rezk-Salama C, editors. *Proc. of Vision, Modeling, and Visualization*; 2010. p. to appear.